

УДК 550.311

THE EFFECT OF POWER-LAW RHEOLOGY OF SURROUNDINGS ON THE GRAVITATIONAL INSTABILITY OF A VISCOUS LAYER

A.T. Ismail-Zadeh¹, H. Huppert²¹International Institute of Earthquake Prediction Theory
and Mathematical Geophysics, Russian Academy of Sciences, Moscow, Russia²Institute of Theoretical Geophysics, University of Cambridge, UK

The gravitational instability of a rheologically stratified system is analyzed in a situation when a buoyant fluid is overlain by a dense perfectly plastic layer and underlain by an infinitely deep layer of a non-Newtonian power-law fluid. The system is subject to depth-dependent horizontal extension or compression. The growth rate of small perturbations versus wavenumber is found in analytical terms. Effects of the viscosity and thickness ratios between the two layers are assessed. The following results are obtained for the case where the viscosity of the buoyant layer is much less than the effective viscosity of surroundings. In contrast to the case of purely viscous layered system, the dominant wavelength of the most unstable mode decreases with increasing thickness of the upper layer. The instability pattern is similar to that of perfectly plastic material. The buckling instability induced by a rapid horizontal straining overwhelms the gravitational instability, and then the growth rate of perturbations depends linearly on the viscosity ratio. The compression of the lower layer reduces the growth rate of the perturbations over a range of wavelengths, and the dominant wavelength becomes longer with increasing compression. The applicability of the analytical results to the problems of salt tectonics is discussed.

ВЛИЯНИЕ СТЕПЕННОЙ РЕОЛОГИИ ОКРУЖАЮЩЕЙ СРЕДЫ НА ГРАВИТАЦИОННУЮ НЕУСТОЙЧИВОСТЬ ВЯЗКОГО СЛОЯ

А.Т. Исмаил-заде¹, Г. Хупперт²¹Международный институт теории прогноза землетрясений
и математической геофизики Российской академии наук, Москва, Россия²Институт теоретической геофизики, Кембриджский университет, Англия

Рассматривается гравитационная неустойчивость реологически стратифицированной системы, в которой вязкий слой пониженной плотности перекрыт более вязким идеально пластическим слоем и находится на полупространстве ньютоновской степенной жидкости. На эту систему действует горизонтальное растяжение или сжатие, изменяющееся с глубиной. Найдены аналитические выражения скорости роста малых возмущений в зависимости от волнового числа. Исследованы эффекты, связанные с изменением контраста вязкости и толщины слоев. Рассматривается случай, когда вязкость легкого слоя много меньше эффективной вязкости других слоев. В противоположность случаю чисто вязких слоев, волновое число максимально нестабильной моды убывает с возрастанием толщины верхнего слоя. Картина неустойчивости аналогична случаю, когда среда идеально пластична. Изгибная неустойчивость, возникающая при быстрой горизонтальной деформации, преобладает над гравитационной неустойчивостью, и в этом случае скорость роста возмущений линейно зависит от контраста вязкости. При сжатии нижнего слоя скорость роста возмущений уменьшается в некотором диапазоне волновых чисел, а при увеличении сжатия длина волны максимальной моды возрастает. Обсуждаются приложения аналитических результатов работы к задачам соляной тектоники.

Introduction

The rheology of sedimentary rocks is quite complex: their properties depend on temperature, composition, pore fluid pressure, and other factors. Because the effective viscosity of the uppermost brittle sediments is rather high, the deformations of rocks are not controlled by dislocation creep and are determined instead by motions of sedimentary blocks along pre-existing faults of various orientations. The dynamic friction at faults depends only very weakly on the strain rate, and such a physical mechanism of deformation is most naturally modeled by the rheology of a strongly non-Newtonian power-law fluid or even perfectly plastic material which does not exhibit work-hardening but flows plastically under constant stress [1].

The gravitational and buckling instabilities are crucial in the evolution of geological structures. The gravitational instability is associated with variations in density due to chemical or thermal heterogeneities. The buckling instability arises from variations of viscosity under the action of an applied stress. These two kinds of instability finally determine whether disturbances will grow or decay in layered structures. When rocksalt is buried under clastic deposits in sedimentary basins, the compacting overburden becomes denser in time than the rocksalt. Salt can then rise through the overlying sedimentary layer to form diapirs [2]. Studies of natural diapirs have benefited from theoretical analyses. Biot [3], Biot and Odé [4], and Ramberg [5] developed a theory of gravitational instability of layered geological media under compression. Schmeling [6] demonstrated how the dominant (but not necessarily characteristic) wavelength and the geometry of the gravity overturns are influenced by the shape of the initial perturbation. Poliakov et al. [7] and Naimark et al. [8] studied numerically the effects of differential loading of sediments on diapirism. In the studies mentioned the layered geological structures were modeled as systems of viscous layers.

We analyze the gravitational instability of a rheologically stratified geological structure under compression or extension and try to explain some features of salt diapirs observed in the sedimentary basin, for example, the non-uniform distribution of diapirs and the reduction of interdiapir spacings. This is in line with recent advances in salt tectonics, which highlight the role of horizontal stretching or squeezing of a brittle overburden in the formation of salt structures [9,10].

Several analytical investigations have been performed to find the differences in growth rates between the instability of Newtonian and non-Newtonian fluids under finite-amplitude compression and extension [11–17]. However these studies either have not addressed the problem of the instability due to density inversion or have not evaluated the features of the instability of rheologically stratified material to determine all implications.

1. Equations of motion and boundary conditions

We study the gravitational instability of a three-layered structure (Fig.1): a perfectly plastic layer of the effective viscosity η_1 and density ρ_1 in $0 \leq z \leq h_1$ overlays a viscous layer of the viscosity η_2 and density ρ_2 in $-h_2 \leq z \leq 0$; both layers rest on an infinitely deep layer filled by a non-Newtonian power-law fluid of the effective viscosity η_3 and density ρ_3 . Hereinafter subscripts 1, 2, and 3 refer to the upper, middle, and lower layers, respectively. The governing equations are represented by the equations of momentum, rheology, continuity, and density advection (see e.g., [18]). Motivated by the extremely large viscosities of geological fluids, we assume that inertial terms in the Navier-Stokes equations are negligible and that the motion is governed by the Stokes equations. In general, the stress tensor τ_{ij} and strain rate tensor $\dot{\epsilon}_{ij}$ satisfy the non-Newtonian power-law fluid relation $\tau_{ij} = C\dot{\epsilon}^{\frac{1-n}{n}}\dot{\epsilon}_{ij}$, where the constant C is defined from thermodynamical conditions, n is the power-law exponent, and $\dot{\epsilon} = (\dot{\epsilon}_{kl}\dot{\epsilon}_{kl})^{1/2}$ is the second invariant of the strain rate.

The structure is subject to layer-parallel extension (or compression) with horizontal strain rates $\dot{\tilde{\epsilon}}_{xx} = \gamma_1$ (or $-\gamma_1$) in the upper layer and $\dot{\tilde{\epsilon}}_{xx} = \gamma_2$ (or $-\gamma_2$) in the lower layer, where γ_1 and γ_2 are constants. Incompressibility implies that $\dot{\tilde{\epsilon}}_{zz} = -\dot{\tilde{\epsilon}}_{xx}$. The remaining component of the strain rate tensor $\dot{\tilde{\epsilon}}_{xz} = 0$ for the background pure shear flow.

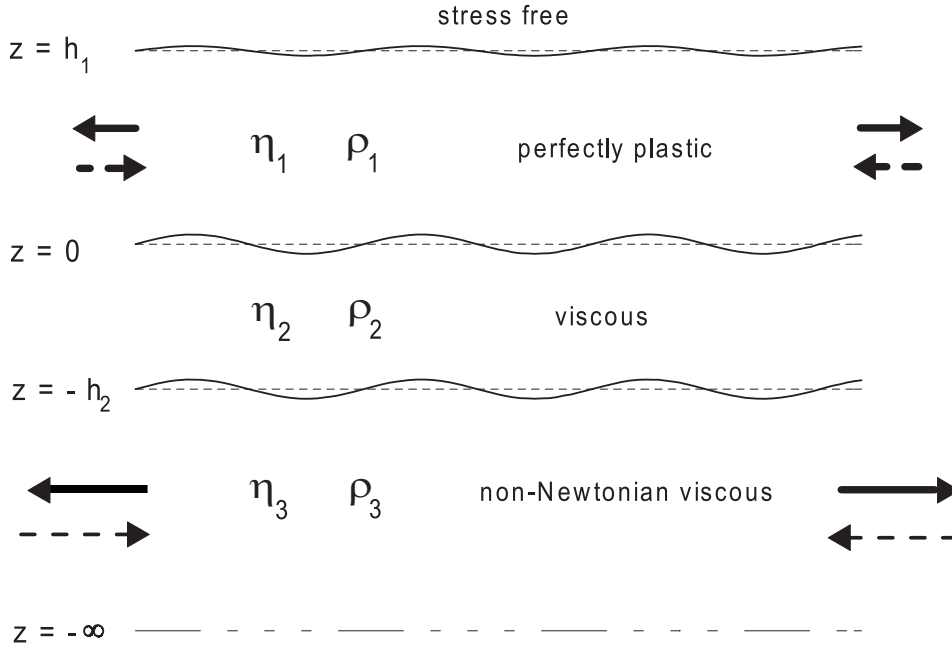


Fig. 1. A sketch of the rheologically layered structure model.

A small sinusoidal perturbation is prescribed to the interfaces of the layers. η_1 and ρ_1 , η_2 and ρ_2 , and η_3 and ρ_3 are the effective viscosity and density of the upper, middle, and lower layers respectively. The layers are subject to horizontal extension or compression of different magnitudes (solid and dashed arrows)

In order to obtain the equations governing the small perturbations of physical variables, we neglect all products and powers of the perturbations and retain only linear terms. We introduce small perturbations of pressure (δP), density ($\delta\rho$), components of velocity \mathbf{v} (u and w), stress tensor, $\delta\tau_{ij}$, and strain-rate tensor ($\delta\dot{\epsilon}_{ij}$). The equations take the form

$$-\frac{\partial\delta P}{\partial x_j} + \frac{\partial\delta\tau_{ij}}{\partial x_j} + \delta\rho F_i = 0, \tag{1}$$

$$\delta\tau_{xx} = 2\frac{\bar{\eta}}{n}\frac{\partial u}{\partial x}, \quad \delta\tau_{zz} = 2\frac{\bar{\eta}}{n}\frac{\partial w}{\partial z}, \quad \delta\tau_{xz} = \bar{\eta}\left(\frac{\partial u}{\partial z} + \frac{\partial w}{\partial x}\right), \tag{2}$$

$$\text{div}\mathbf{v} = 0, \tag{3}$$

$$\frac{\partial\delta\rho}{\partial t} + w\frac{d\rho}{dz} = 0, \tag{4}$$

where $i, j = x, z$; $F_i = (0, -g)$; and $\bar{\eta}$ is the effective viscosity defined to be $0.5C\dot{\epsilon}^{\frac{1-n}{n}}$. Equation (2) represents the anisotropic stress–strain rate relationships in the case of the non-Newtonian power-law rheology (e.g., [11]).

The conditions at the upper boundary $z = h_1$ are stress-free and obtained from the absence of tangential and normal stress

$$\delta\tau_{xz,1} = \bar{\sigma}_{xx,1}\frac{\partial\zeta}{\partial x}, \tag{5}$$

$$-\delta P_1 + \delta\tau_{zz,1} + \rho_1 g\zeta = 0, \tag{6}$$

where $\bar{\sigma}_{xx,1} = 4\eta_1\bar{\epsilon}_{xx,1} = 4\eta_1\gamma$ is the component of stress tensor for the basic background flow [12], and ζ is the vertical displacement of the upper boundary defined by $\partial\zeta/\partial t = w_1$.

At the interfaces between the upper and middle layers ($z = 0$) and the middle and lower layers ($z = -h_2$), we require continuity of velocity, tangential and normal stress accounting for forces due to the density and viscosity discontinuities at the interface

$$u_i = u_{i+1}, \quad w_i = w_{i+1}, \quad (7)$$

$$\delta\tau_{xz,i} - \delta\tau_{xz,i+1} = (\bar{\sigma}_{xx,i} - \bar{\sigma}_{xx,i+1}) \frac{\partial \xi_i}{\partial x}, \quad (8)$$

$$-\delta P_i + \delta P_{i+1} + \delta\tau_{zz,i} - \delta\tau_{zz,i+1} - (\rho_{i+1} - \rho_i)g\xi_i = 0. \quad (9)$$

where $\partial \xi_i / \partial t = w_i = w_{i+1}$ and $i = 1, 2$. Equations (5) and (8) include the driving mechanism for the background flow induced by extension or compression, while the last term in (6) and (9) provides the motion of the layered structure due to density discontinuity.

Analyzing the disturbance into normal modes, we use the Laplace-Fourier transform with the kernel $\exp(ikx + pt)$, where k is the wavenumber and p is the growth rate of the perturbations. The stability problem then reduces to the analysis of variable p as a function of k . If all p have negative real part for all k , then the system of layers is stable; the system is unstable if there exist p with a positive real part for some range of k . For solutions having this dependence on x and t , (1)–(4) become

$$ik\delta P = -\frac{2\bar{\eta}}{n}k^2u + D[\bar{\eta}(Du + ikw)], \quad (10)$$

$$D\delta P = ik[\bar{\eta}(Du + ikw)] + D\left(\frac{2\bar{\eta}}{n}Dw\right) - g\delta\rho, \quad (11)$$

$$iku + Dw = 0, \quad (12)$$

$$p\delta\rho = -wD\rho, \quad (13)$$

where $D = d/dz$. We multiply (10) by ik , use (12) and combine (11) and (13) to obtain

$$-k^2\delta P = \frac{2\bar{\eta}}{n}k^2Dw - D[\bar{\eta}(D^2 + k^2)w], \quad (14)$$

$$D\delta P = -\bar{\eta}(D^2 + k^2)w + D\left(\frac{2\bar{\eta}}{n}Dw\right) + \frac{gD\rho}{p}w. \quad (15)$$

Eliminating δP between (14) and (15), we obtain

$$(D^2 + k^2)(\bar{\eta}(D^2 + k^2)w) - 4k^2D\left(\frac{\bar{\eta}}{n}Dw\right) - \frac{gD\rho}{p}w = 0. \quad (16)$$

We assume the density and viscosity to be constant within each layer. Then (16) becomes

$$\left\{(D^2 + k^2)^2 - \frac{4k^2}{n}D^2\right\}w = 0. \quad (17)$$

The general solution to (17) is the linear combination

$$w = A_3 \exp(k\beta_1 z) + B_3 \exp(k\beta_2 z) + C_3 \exp(k\beta_3 z) + D_3 \exp(k\beta_4 z), \quad (18)$$

where A_3, B_3, C_3 , and D_3 are constants and

$$\beta_j = \pm \left\{ \frac{2}{n} - 1 \pm i \frac{2(1-n)^{\frac{1}{2}}}{n} \right\}^{\frac{1}{2}} \quad (j = 1, 2, 3, 4).$$

In the case of a Newtonian fluid ($n = 1$) (17) becomes

$$(D^2 - k^2)^2 w = 0 \quad (19)$$

with the general solution

$$w = A_2 \cosh kz + B_2 \sinh kz + C_2 z \cosh kz + D_2 z \sinh kz, \quad (20)$$

where A_2, B_2, C_2 , and D_2 are constants.

In a case of a perfectly plastic medium ($n = \infty$) (17) becomes

$$(D^2 + k^2)^2 w = 0 \tag{21}$$

with the general solution

$$w = A_1 \cos kz + B_1 \sin kz + C_1 z \cos kz + D_1 z \sin kz, \tag{22}$$

where A_1, B_1, C_1 , and D_1 are constants.

Boundary conditions (5)–(9) are represented in the form:

$$\left(D^2 + k^2 - \frac{4\gamma k^2}{p} \right) w_1 = 0, \tag{23}$$

$$\left(D + \frac{1}{k^2} D^3 - \frac{\rho_1 g}{\eta_1 p} \right) w_1 = 0, \tag{24}$$

$$w_1 = w_2, \quad D w_1 = D w_2, \tag{25}$$

$$(D^2 + k^2) w_1 = \frac{\eta_2}{\eta_1} (D^2 + k^2) w_2 + \frac{4\gamma_1 k^2}{p} \left(1 - \frac{\eta_2}{\eta_1} \right) w_2, \tag{26}$$

$$- \left(\frac{1}{k^2} D^3 + D \right) w_1 + \frac{\eta_2}{\eta_1} \left(\frac{1}{k^2} D^3 - 3D \right) w_2 = \frac{(\rho_2 - \rho_1)g}{\eta_1 p} w_2, \tag{27}$$

$$w_2 = w_3, \quad D w_2 = D w_3, \tag{28}$$

$$\frac{\eta_2}{\eta_3} (D^2 + k^2) w_2 = (D^2 + k^2) w_3 + \frac{2k^2}{p} \left(\gamma_1 \frac{\eta_2}{\eta_3} - \gamma_2 \right) w_3, \tag{29}$$

$$- \frac{\eta_2}{\eta_3} \left(\frac{1}{k^2} D^3 - 3D \right) w_2 + \left(\frac{1}{k^2} D^3 - \frac{1}{3} D \right) w_3 = \frac{(\rho_3 - \rho_2)g}{\eta_3 p} w_3. \tag{30}$$

2. Linear analysis

Equations (21) for the upper layer, (19) for the middle layer, and (17) for the lower layer ($n = 3$) with boundary conditions (23)–(30) make the boundary value problem for the eigenvalue p and eigenfunction w . The conditions of no flow as $z \rightarrow -\infty$ reduce solution (18) of equation (17) to the form

$$w = \exp(kaz) (A_3 \cos kbz + B_3 \sin kbz), \tag{31}$$

$$a = \cos \frac{\varphi}{2}, \quad b = \sin \frac{\varphi}{2}, \quad \varphi = \arccos(-1/3).$$

Substituting solutions (20), (22), and (31) into the boundary conditions, we obtain a system of ten linear algebraic equations for ten constants A_k, B_k, C_l , and D_l ($k = 1, 2, 3, l = 1, 2$). Zeros of the determinant, of this linear system are eigenvalues of the boundary value problem.

We introduce the following dimensionless quantities ($i = 1, 2, 3, j = 1, 2$)

$$\begin{aligned} a_i &= \eta_i / (\eta_1 + \eta_2), \quad c_i = \rho_i / (\rho_1 + \rho_2), \\ \nu_1 &= \eta_2 / \eta_1 = a_2 / a_1, \quad \nu_2 = \eta_2 / \eta_3 = a_2 / a_3, \\ d_j &= h_j / (h_1 + h_2), \quad q = k(h_1 + h_2), \quad x_j = qd_j = kh_j, \\ \lambda &= pt_0, \quad \bar{\gamma}_j = 2\gamma_j t_0, \quad \mathcal{F} = \frac{(\rho_1 + \rho_2)g(h_1 + h_2)t_0}{2(\eta_1 + \eta_2)}, \\ \mathcal{G}_1 &= \mathcal{F}c_1 d_1 / a_1, \quad \mathcal{G}_{21} = \mathcal{F}(c_2 - c_1)d_2 / a_1, \quad \mathcal{G}_{32} = \mathcal{F}(c_3 - c_2)d_2 / a_3. \end{aligned}$$

After some manipulation, we deduce that a nontrivial solution to the above linear algebraic equations exists when

$$\det(p_{ij}) = 0 \tag{32}$$

where

$$\begin{aligned}
p_{11} &= \lambda \left(\frac{\mathcal{G}_{21}}{x_2} \tan x_1 + \bar{\gamma}_1 \nu_1 \right) + \bar{\gamma}_1 \left(\frac{\mathcal{G}_{21}}{x_2} (x_1 - \tan x_1) + \bar{\gamma}_1 (1 - \nu_1) x_1 \tan x_1 \right), \\
p_{12} &= \nu_1 (\bar{\gamma}_1 x_1 + (\lambda - \bar{\gamma}_1) \tan x_1), \quad p_{13} = \bar{\gamma}_1 \tan x_1, \quad p_{14} = \nu_1 (\bar{\gamma}_1 x_1 \tan x_1 - \lambda), \\
p_{21} &= \lambda \left(\frac{\mathcal{G}_{21}}{x_2} x_1 + \mathcal{G}_1 + \bar{\gamma}_1 (1 - \nu_1) x_1 \tan x_1 \right) \\
&\quad + \mathcal{G}_1 \left(\frac{\mathcal{G}_{21}}{x_2} (x_1 - \tan x_1) + \bar{\gamma}_1 (1 - \nu_1) x_1 \tan x_1 \right), \\
p_{22} &= \nu_1 ((\mathcal{G}_1 + \lambda) x_1 - \mathcal{G}_1 \tan x_1), \quad p_{23} = \mathcal{G}_1 \tan x_1, \\
p_{24} &= \nu_1 (\mathcal{G}_1 + \lambda) x_1 \tan x_1, \quad p_{15} = p_{16} = p_{25} = p_{26} = 0, \\
p_{31} &= \cosh x_2 - x_2 \sinh x_2, \quad p_{32} = -\sinh x_2 + x_2 \cosh x_2, \\
p_{33} &= -x_2 \cosh x_2, \quad p_{34} = x_2 \sinh x_2, \quad p_{35} = 1, \quad p_{36} = 0, \\
p_{41} &= x_2 \cosh x_2, \quad p_{42} = -x_2 \sinh x_2, \quad p_{43} = \cosh x_2 + x_2 \sinh x_2, \\
p_{44} &= -(\sinh x_2 + x_2 \cosh x_2), \quad p_{45} = a, \quad p_{46} = -b, \\
p_{51} &= -\nu_2 x_2 \sinh x_2, \quad p_{52} = \nu_2 x_2 \cosh x_2, \\
p_{53} &= -\nu_2 (\sinh x_2 + x_2 \cosh x_2), \quad p_{54} = \nu_2 (\cosh x_2 + x_2 \sinh x_2), \\
p_{55} &= \frac{1}{2} (a^2 - b^2 - 1) + \frac{1}{\lambda} (\nu_2 \bar{\gamma}_1 - \bar{\gamma}_2), \quad p_{56} = -ab, \\
p_{61} &= -\nu_2 (\sinh x_2 - x_2 \cosh x_2), \quad p_{62} = \nu_2 (\cosh x_2 - x_2 \sinh x_2), \\
p_{63} &= \nu_2 x_2 \sinh x_2, \quad p_{64} = -\nu_2 x_2 \cosh x_2, \\
p_{65} &= -\frac{1}{2} a (a^2 - 3b^2 - \frac{1}{3}) + \frac{\mathcal{G}_{32}}{x_2 \lambda}, \quad p_{66} = \frac{1}{2} b (3a^2 - b^2 - \frac{1}{3}).
\end{aligned}$$

Equation (32) is a cubic polynomial with respect to the growth rate λ associated with the induced background flow and a flow due to density discontinuity. We do not present here the coefficients of the polynomial for the lack of space. We find roots of the cubic polynomial from the Cardano formula. We consider the maximum positive root for λ , that is, the least stable root. It should be noted that signs of two roots of (32) may exchange for some values of q , ν_1 , ν_2 , $\bar{\gamma}_1$, and $\bar{\gamma}_2$.

To illustrate the results, we take the following values of the model parameters: $h_1 + h_2 = 10$ km; $\mu_1 + \mu_2 = 2 \times 10^{20}$ Pa s; $\rho_1 = 2.5 \times 10^3$ kg m $^{-3}$, $\rho_2 = 2.2 \times 10^3$ kg m $^{-3}$, and $\rho_3 = 2.7 \times 10^3$ kg m $^{-3}$; $t_0 = 3 \times 10^{13}$ s. These values model rocksalt overlain by a sedimentary overburden and underlain by a subsalt layer.

First, we analyze the case when the horizontal background strain rates, $\bar{\gamma}_1$ and $\bar{\gamma}_2$, are small to inhibit the development of the buckling instability. We find that $\bar{\gamma}_0 = 10^{-6}$ is a reasonable value of the background strain rate in this case. For such small values of the strain rate gravity effects dominate in the instability of the layered structure. When $c_1 > c_2$ and both $\bar{\gamma}_1 < \bar{\gamma}_0$ and $\bar{\gamma}_2 < \bar{\gamma}_0$, at least one of the roots of (32) is positive for all q . Fig.2 illustrates the curves of the growth rate versus wavenumber for various values of effective viscosity ratio ν_1 .

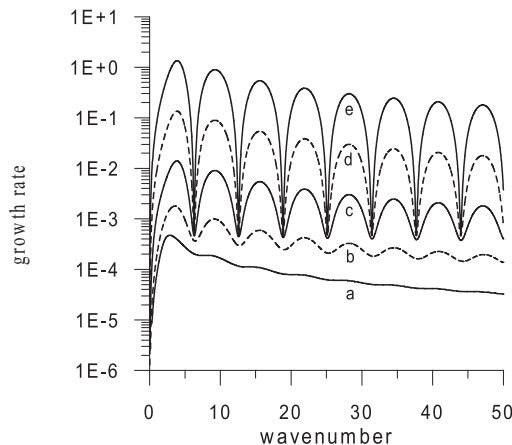


Fig. 2. The growth rate versus wavenumber for various values of the effective viscosity ratio, ν_1 : 1 (a), 0.1 (b), 10^{-2} (c), 10^{-3} (d), and 10^{-4} (e), at $d_1/d_2 = 1$, $c_1 - c_2 = 0.06$, $c_3 - c_2 = 0.1$, $\nu_2 = 10^{-4}$, and $\bar{\gamma}_1 = \bar{\gamma}_2 = 10^{-7}$.

We see that the smaller effective viscosity ratio, the higher a positive growth rate and the larger an amplitude of the curve waviness. The waviness of growth rate curves is due to the fact that the perturbation equation for perfectly plastic material is a hyperbolic wave equation and the vertical velocity structure $w(z)$ is oscillatory.

The dominant wavenumber initially decreases with increasing thickness ratio but then increases again by a series of abrupt jumps (Fig.3, left panel). This behavior is associated with the waviness of the growth rate curve and hence is due to the non-Newtonian rheology of the upper and lower layers. It occurs when the second, third and so on peaks of the growth rate curve becomes higher than the surrounding peaks. The maximum growth rate initially increases with increasing thickness ratio; however, it decreases steadily for larger thickness ratio (Fig.3, right panel).

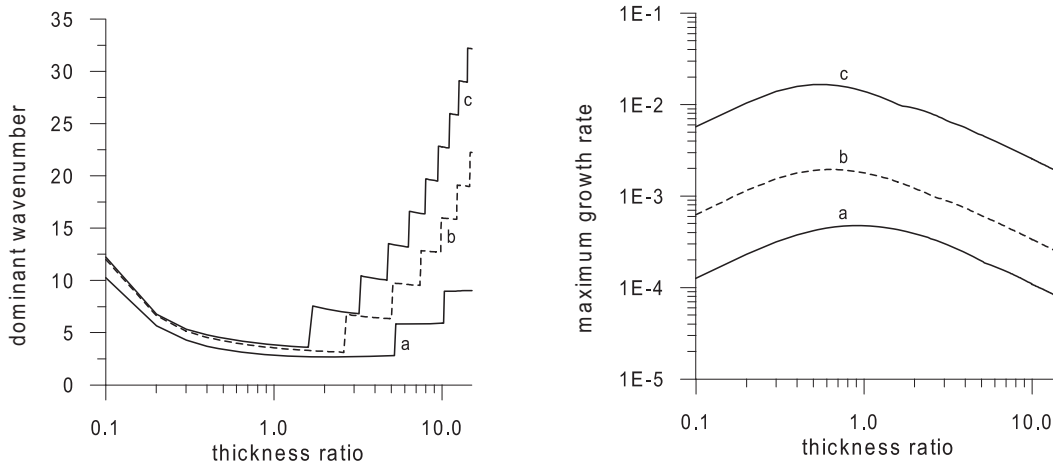


Fig. 3. The dominant wavenumber (left panel) and maximum growth rate (right panel) versus the thickness ratio, d_1/d_2 , for various values of the effective viscosity ratio, ν_1 : 1 (a), 0.1 (b), and 10^{-2} (c), at $c_1 - c_2 = 0.06$, $c_3 - c_2 = 0.1$, $\nu_2 = 10^{-4}$, and $\bar{\gamma}_1 = \bar{\gamma}_2 = 10^{-7}$

Fig.4 illustrates growth rate curves for both horizontal extension (curves *a-d*) and compression (curves *e-h*) of the upper layer while the background strain rate $\bar{\gamma}_2 < \bar{\gamma}_0$. It shows the growth rates to be positive for small values of background strain rate $\bar{\gamma}_1$ and to become either positive or negative for larger $\bar{\gamma}_1$. The maximum growth rate increases in amplitude with increasing background strain rate $\bar{\gamma}_1$, while the other sinusoidal peaks of the growth rate curves increase faster and become dominant. At large background strain rates ($\bar{\gamma}_1 > 10^{-5}$) the model tends to a "resonance" behaviour marked by sinusoidal growth rate curves and by a linear dependence of the rate on effective viscosity ratio [13].

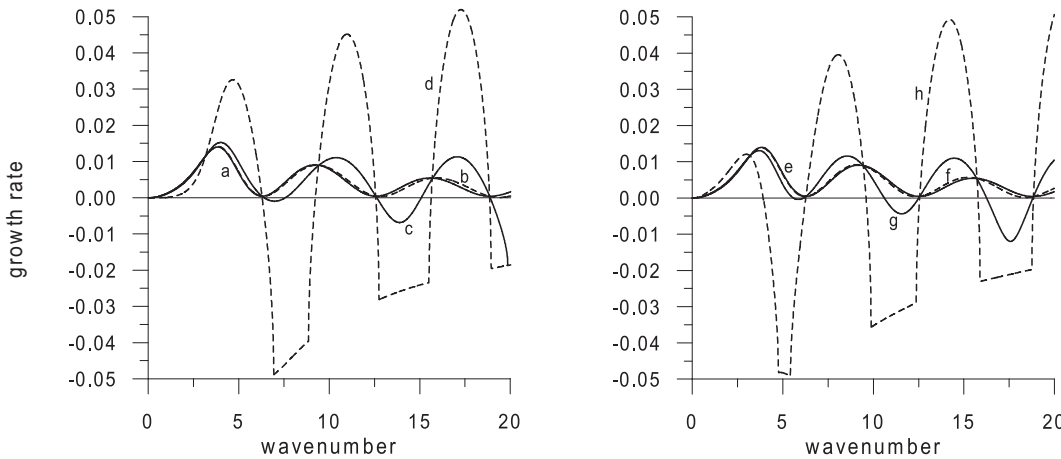


Fig. 4. The growth rate versus wavenumber for various values of the basic background strain rate $\bar{\gamma}_1$. For extension: 10^{-7} (a), 10^{-6} (b), 10^{-5} (c), 10^{-4} (d); for compression: -10^{-7} (e), -10^{-6} (f), -10^{-5} (g), -10^{-4} (h), all at $d_1/d_2 = 1$, $c_1 - c_2 = 0.06$, $c_3 - c_2 = 0.1$, $\nu_2 = 10^{-4}$, and $\bar{\gamma}_2 = 10^{-7}$

Curves in Fig. 5 show how the maximum growth rate depends on horizontal extension or compression of the lower layer at $\bar{\gamma}_1 < \bar{\gamma}_0$ and $\nu_1 = \nu_2 = 0.1$. At small wavenumbers (or at long wavelengths) the growth rate is seen to fall down with decreasing strain rate $\bar{\gamma}_2$. Large compression of the lower layer retards the growth of perturbations for wavenumbers less than 6 and finally results in a negative growth rate at some interval of wavenumbers ranged from about 1 to 4 and increasing growth rate for wavenumbers less than about 1. It was also found that changes in $\bar{\gamma}_2$ have little effect on the growth rate curves for large wavenumbers. If the effective viscosity ratios ν_1 and ν_2 are sufficiently small, much larger compression of the lower layer (than that in the case of $\nu_1 = \nu_2 = 0.1$) is required to shift the dominant wavenumber to small values.

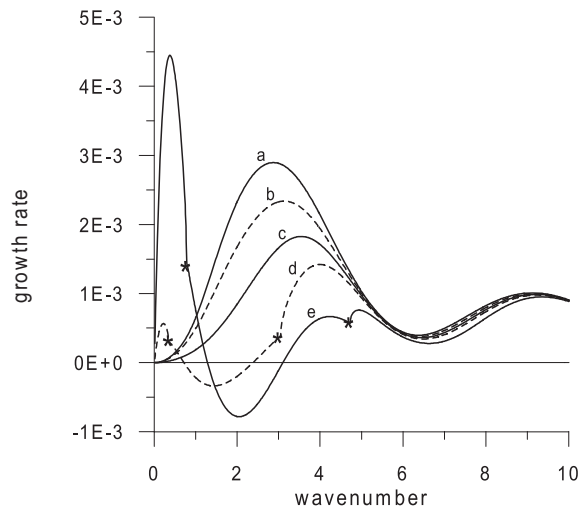


Fig. 5. The growth rate versus wavenumber for various values of the basic background strain rate, $\bar{\gamma}_2$: 10^{-2} (a), 5×10^{-3} (b), 10^{-7} (c), -10^{-2} (d), -2×10^{-2} (e), at $\nu_1 = \nu_2 = 0.1$, $d_1/d_2 = 1$, $c_1 - c_2 = 0.06$, $c_3 - c_2 = 0.1$, and $\bar{\gamma}_1 = 10^{-7}$. Asterisks show points of sign exchange between two roots of Eq.(32)

The results of the analytical study show that when the viscosity of the middle layer is less than the effective viscosity of surroundings, the instability of the structure under compression or extension is similar to the instability of perfectly plastic material manifested as oscillations of the growth rate curves and a linear dependence of the growth rates on effective viscosity ratio.

Discussion and conclusions

We studied the gravitational instability of a rheologically layered structure under compression or extension and analyzed the growth rates and dominant wavelengths of the perturbations generated in the structure. During a deposition of sediments the thickness of the salt overburden grows with respect to the initial thickness of the salt layer. Assuming the sedimentation to be rapid compared to the timescale of diapirism, the distance between the crests of two neighboring diapirs is defined by the dominant wavelength. The analytical results show that the dominant wavelength is short when the overburden is rather thin. Initially it becomes longer with increasing thickness of the overburden but then reduces when the thickness of the overburden becomes greater than the thickness of the salt layer. Such a reduction of the dominant wavelength can explain the surprisingly small distance between salt diapirs in some sedimentary basins (for example, in the Great Kavir in Iran, see [19]).

The extension of sedimentary layers containing salt results in the thinning of a brittle overburden, its faulting, and the activation of salt diapirs (e.g., [20]). We showed that the buckling instability replaces the gravitational instability for rather rapid horizontal stretching or squeezing of the rheologically layered structure. We demonstrated that the modes of instability associated with the waviness of growth rate curves have much the same growth rate. It means that the induced background flow may generate a mixture of diapirs with different wavelengths rather than diapirs with one dominant wavelength associated with a well-defined maximum growth rate. This provides a possible origin for a non-uniform distribution of mature diapirs.

Depth-dependent strain rate is one of the factors influencing the formation of layered structures. A thin-skinned and thick-skinned extension or compression can result in different way of evolution of salt diapirs [9,20]. Our model of three-layered structure can be applied to analyze the evolution of salt diapirs overlain by a perfectly plastic overburden and underlain by a non-Newtonian subsalt layer. The model results show that the growth rate of the instability and the dominant wavelength can significantly change for large compression of the subsalt layer.

Although real rocks display more complex rheology than a strongly non-Newtonian fluid, we consider our study of particular situations as an essential step in understanding the dynamics of rheologically stratified natural structures. We conclude, on theoretical grounds, that the rheologically layered system yields plastically for small values of the ratio between the viscosity of the middle layer and the effective viscosity of its surroundings.

We are very thankful to J.R. Lister, B.M. Naimark, and C.J. Talbot for their constructive comments. The research was supported by the Royal Society of London, the U.S. National Science Foundation (EAR-9804859), the International Science and Technology Center (project 1293-99), the Russian Foundation of Basic Research (99-05-65050) and the Fellowship of the President of the Russian Federation to Young Doctors of Science (99-15-96085).

REFERENCES

1. *Prager W., Hodge P.* Theory of Perfectly Plastic Solids. London: Chapman & Hall, 1951. 264 p.
2. *Talbot C.J., Rönnlund P., Schmeling H., Koyi H., Jackson M.P.A.* Diapiric spoke patterns // *Tectonophysics*. 1991. Vol.188. P.187–201.
3. *Biot M.A.* Theory of viscous buckling and gravity instability of multilayers with large deformation // *Geol. Soc. Amer. Bull.* 1965. Vol.76. P.371–378.
4. *Biot M.A., Odé. H.* Theory of gravity instability with variable overburden and compaction // *Geophysics*. 1965. Vol.30. P.213–227.
5. *Ramberg H.* Instability of layered system in the field of gravity // *Phys. Earth Planet. Inter.* 1968. Vol.1. P.427–474.
6. *Schmeling H.* On the relation between initial conditions and late stages of Rayleigh-Taylor instabilities // *Tectonophysics*. 1987. Vol.133. P.65–80.
7. *Poliakov A., van Balen R., Podladchikov Yu., Daudre B., Cloetingh S., Talbot C.* Numerical analysis of how sedimentation and redistribution of surficial sediments affects salt diapirism // *Tectonophysics*. 1993. Vol.226. P.199–216.
8. *Naimark B.M., Ismail-Zadeh A.T., Jacoby W.R.* Numerical approach to problems of gravitational instability of geostructures with advected material boundaries // *Geophys. J. Inter.* 1998. Vol.134. P.473–483.
9. *Vendeville B.C., Jackson M.P.A.* A rise of diapirs during thin-skinned extensions // *Marine Petrology and Geology*. 1992. Vol.9. P.331–353.
10. *Jackson M.P.A., Vendeville B.C.* Regional extension as a geological trigger for diapirism // *Geol. Soc. Amer. Bull.* 1994. Vol.106. P.57–73.
11. *Fletcher R.C.* Wavelength selection in the folding of a single layer with power-law rheology // *Amer. J. Sci.* 1974. Vol.274. P.1029–1043.
12. *Smith R.B.* Formation of folds, boudinage, and mullions in non-Newtonian materials // *Geol. Soc. Amer. Bull.* 1977. Vol.88. P.312–320.
13. *Smith R.B.* The folding of a strongly non-Newtonian layer // *Amer. J. Sci.* 1979. Vol.279. P.272–287.
14. *Ricard Y., Froidevaux C.* 1986 Stretching instability and lithospheric boudinage // *J. Geophys. Res.* 1986. Vol.91. P.8314–8324.
15. *Martinod J., Davy P.* Periodic instability during compression or extension of the lithosphere 1. Deformation modes from an analytical perturbation method // *J. Geophys. Res.* 1992. Vol.97. P.1999–2014.
16. *Birger B.I.* Stability of the lithosphere during horizontal compression (in Russian) // *In Modern Problems of Seismology and Geodynamics* Eds. V.I. Keilis-Borok and G.M. Molchan. Moscow: Nauka, 1996. P.3–21.
17. *Conrad C.P., Molnar P.* The growth of Rayleigh-Taylor instability in the lithosphere for various rheological and density structures // *Geophys. J. Inter.* 1997. Vol.129. P.95–112.
18. *Chandrasekhar S.* Hydrodynamic and Hydromagnetic Stability. Oxford University Press. 1961. 654 p.
19. *Jackson M.P.A., Cornelius R.R., Craig C.H., Gansser A., Stocklin J., Talbot C.J.* Salt diapirs of the Great Kavir, Central Iran // *Geol. Soc. Amer. Mem.* 1990. Vol.177. 139 p.
20. *Jackson M.P.A. and Talbot C.J.* Advances in salt tectonics. In *Continental Deformation* / Ed. P.L. Hancock. Pergamon Press, 1994. P.159–179.